

Cite this: *New J. Chem.*, 2012, **36**, 1541–1544

www.rsc.org/njc

LETTER

Ag₃PO₄/SnO₂ semiconductor nanocomposites with enhanced photocatalytic activity and stability†

Lili Zhang,‡ Hengchao Zhang,‡ Hui Huang, Yang Liu* and Zhenhui Kang*

Received (in Montpellier, France) 16th March 2012, Accepted 7th May 2012

DOI: 10.1039/c2nj40206h

Ag₃PO₄/SnO₂ semiconductor nanocomposites exhibit much higher photocatalytic activity and good stability than pure Ag₃PO₄ for the photodegradation of organic compounds (methyl orange) in the absence of electron acceptors under visible light.

Intense research has been devoted to searching for suitable semiconductor based photocatalysts due to their applications in solving environmental pollution and solar energy conversion utilizing the energy of either natural sunlight or artificial indoor illumination.^{1–6} More recently, a great breakthrough was made by Yi and co-workers, who reported a new use of Ag₃PO₄ semiconductor,^{7–9} which can make full use of visible light (up to 90%) for O₂ evolution from water as well as great photodecomposition of organic compounds. However, Ag₃PO₄ is slightly soluble in aqueous solution, which greatly reduces its structural stability.⁷ Unfortunately, the photocatalytic process is usually accompanied by the transformation of Ag⁺ into Ag, resulting in the photocorrosion of Ag₃PO₄ in the absence of electron acceptors.⁹ Therefore, it is still a huge challenge to develop a facile and efficient way to modify the stability of Ag₃PO₄ photocatalyst and maintain or enhance its activity without using sacrificial reagents.⁹

The photocatalytic activity of a semiconductor is strongly dependent on the transport and separation efficiencies of photo-generated electrons and holes in the photocatalysts.^{10–12} However, free charge carriers (free electrons and holes) are easily trapped or scattered by various kinds of random defects, resulting in increasing recombination probability. Therefore, promoting the separation of photogenerated electrons and holes will facilitate the photocatalytic process. SnO₂, a direct wide band gap n-type semiconductor ($E_g = 3.8$ eV) with outstanding electrical and optical properties, has been widely applied to gas sensing, electrocatalysts, photocatalysts, and lithium electrodes.^{13–16} Recently, many efforts have been devoted to the controlled synthesis of SnO₂-semiconductor

nanocomposites with suitable valence band and conduction band positions (such as SnO₂/TiO₂, SnO₂/ZnO, SnO₂/Fe₂O₃, etc.)^{17–19} to effectively decrease the probability of electron–hole recombination and enhance the photocatalytic activities. The hybrid nanoparticles have shown novel optical or catalytic properties compared with their individual single-component materials. Considering these great merits of SnO₂-based complex photocatalysts and the limitations of the Ag₃PO₄ photocatalytic system, the combination of SnO₂ and Ag₃PO₄ may be regarded as an ideal strategy to construct a stable and efficient complex photocatalytic system.

Herein, we report the facile one-step fabrication of Ag₃PO₄/SnO₂ composites, which were demonstrated to show improved photocatalytic performance and structural stability for the photodecomposition of organic compounds (methyl orange) under visible light. Accordingly, a reasonable model is proposed to illustrate the key roles of SnO₂ in the photocatalytic process. It is noteworthy that this is the first report regarding the Ag₃PO₄/SnO₂ semiconductor composites for organic compounds under visible light.

To reveal the role of SnO₂ in improving and stabilizing the photocatalytic activity of Ag₃PO₄ complex system, rhombic dodecahedral-like Ag₃PO₄ nanoparticles with relatively smooth surface and average diameter of *ca.* 800 nm were fabricated for comparison (Fig. S1†). Ag₃PO₄/SnO₂ composites were synthesized by simply reacting CH₃COOAg with Na₂HPO₄ in Na₂SnO₃·3H₂O aqueous solution at room temperature (see ESI† for experimental details). Fig. 1a shows the scanning electron microscopy (SEM) image of the obtained Ag₃PO₄/SnO₂ composite photocatalysts, revealing the rhombic dodecahedral morphology was maintained for the composite with uniform size about 700–800 nm.

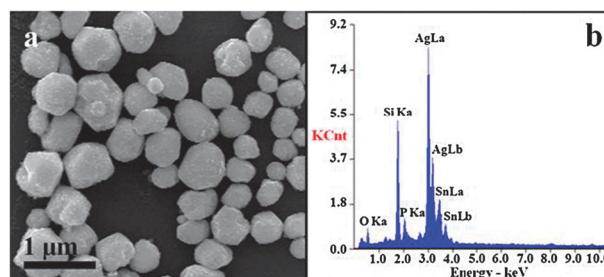


Fig. 1 (a) SEM images and (b) EDS patterns of Ag₃PO₄/SnO₂ complex photocatalyst.

Institute of Functional Nano & Soft Materials (FUNSOM) and Jiangsu Key Laboratory for Carbon-Based Functional Materials & Devices, Soochow University, Suzhou, China.

E-mail: yangl@suda.edu.cn, zhkang@suda.edu.cn

† Electronic supplementary information (ESI) available: Experimental procedures; SEM images of Ag₃PO₄. See DOI: 10.1039/c2nj40206h

‡ These authors contributed equally to this work.

Energy dispersive X-ray (EDS) pattern of $\text{Ag}_3\text{PO}_4/\text{SnO}_2$ composite photocatalysts was also recorded and shown in Fig. 1b, where signals from Sn, Ag, P, and O were detected.

Fig. 2a shows the transmission electron microscopy (TEM) image of the obtained $\text{Ag}_3\text{PO}_4/\text{SnO}_2$ composite photocatalysts. The distinct contrast between the Ag_3PO_4 particles and the SnO_2 surface layer (the thickness is about 20 nm) confirms the formation of $\text{Ag}_3\text{PO}_4/\text{SnO}_2$ composites, and the SnO_2 surface layer is composed of SnO_2 nanoparticles and not a compact layer. To further confirm the formation of the $\text{Ag}_3\text{PO}_4/\text{SnO}_2$ complex structure, a high-resolution transmission electron microscopy (HRTEM) image was recorded and shown in Fig. 2b. The interplanar spacings of 0.335 and 0.264 nm were clearly observed, which correspond to (110) and (101) crystallographic planes of SnO_2 , respectively, in good agreement with the card JCPDS No. 41-1445.

X-Ray diffraction (XRD) patterns in Fig. 3 give further support to different crystalline structures of the as-synthesized Ag_3PO_4 and $\text{Ag}_3\text{PO}_4/\text{SnO}_2$ samples. For line a, all the characteristic diffraction peaks marked by “▼” can be readily indexed as the different crystalline planes of Ag_3PO_4 (JCPDS No. 06-0505). Compared to the pure Ag_3PO_4 crystals, except for the peaks of Ag_3PO_4 , the diffraction peaks marked by “◇” in line b can be readily indexed as the (110), (101) and (211) planes of SnO_2 (JCPDS No. 41-1445), respectively, confirming the formation of $\text{Ag}_3\text{PO}_4/\text{SnO}_2$ composite. The UV-vis absorption spectra of the as-synthesized samples are shown in Fig. S2†. The absorption edges of Ag_3PO_4 in the $\text{Ag}_3\text{PO}_4/\text{SnO}_2$ sample shift blue slightly, indicating the introduction of small quantity of SnO_2 ($E_g = 3.8$) nanoparticles.^{20,21}

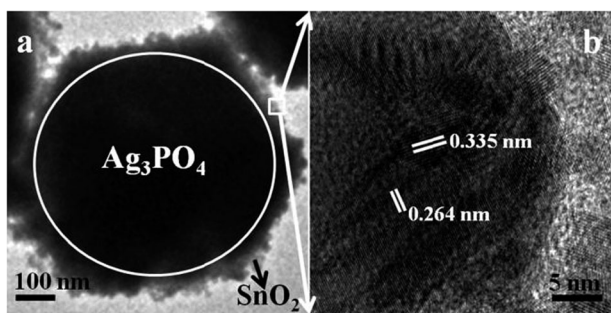


Fig. 2 (a) TEM and (b) HRTEM images of $\text{Ag}_3\text{PO}_4/\text{SnO}_2$ composite photocatalyst.

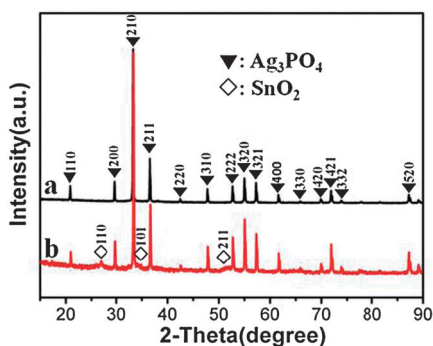


Fig. 3 XRD patterns of (a) Ag_3PO_4 and (b) $\text{Ag}_3\text{PO}_4/\text{SnO}_2$ photocatalysts.

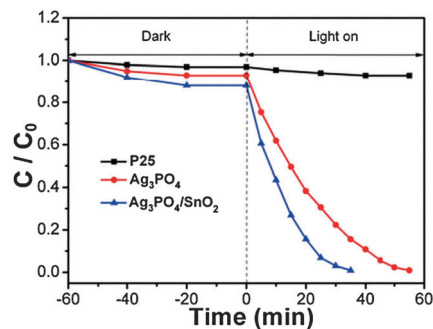


Fig. 4 Photocatalytic activities of P25, Ag_3PO_4 and $\text{Ag}_3\text{PO}_4/\text{SnO}_2$ for MO degradation under visible-light ($\lambda \geq 420$ nm) irradiation.

In the experiments, pure Ag_3PO_4 was used as a photocatalytic reference to qualitatively understand the photocatalytic activity of $\text{Ag}_3\text{PO}_4/\text{SnO}_2$ photocatalysts. The as-synthesized photocatalysts were explored for the degradation of methyl orange (MO) dye under visible light ($\lambda \geq 420$ nm) irradiation and with non-sacrificial reagents at room temperature. Fig. 4 shows the degradation rates of MO dye over P25, Ag_3PO_4 and $\text{Ag}_3\text{PO}_4/\text{SnO}_2$ photocatalysts, respectively. We can see that $\text{Ag}_3\text{PO}_4/\text{SnO}_2$ exhibit the higher photocatalytic activity than pure Ag_3PO_4 , while P25 do not show evident photocatalytic ability for the degradation of MO under the same irradiation conditions. For $\text{Ag}_3\text{PO}_4/\text{SnO}_2$ the complete degradation of the MO dye takes about 35 min, whereas, in the case of pure Ag_3PO_4 , the complete degradation of the MO dye takes about 55 min. These results clearly demonstrate that introducing SnO_2 into Ag_3PO_4 photocatalyst system can greatly enhance their photocatalytic activity.

In addition to photocatalytic activity, the stability of photocatalysts is another important issue for their practical applications. Therefore, we studied the crystalline structures of Ag_3PO_4 and $\text{Ag}_3\text{PO}_4/\text{SnO}_2$ after the MO photodegradation experiments to evaluate their structural stability. Fig. 5a shows the XRD patterns of Ag_3PO_4 and $\text{Ag}_3\text{PO}_4/\text{SnO}_2$ photocatalysts after 10 MO decomposition experiments. It can be clearly seen from line a that after the photodegradation experiment diffraction peaks readily indexed as the (111), (200) and (220) planes of metallic silver (marked by “★”) emerged in the XRD pattern of pure Ag_3PO_4 , indicating that partial reduction of Ag_3PO_4 into metallic Ag particles had taken place during the MO degradation process. Amazingly, no evident crystalline structure changes could be observed in the XRD pattern of $\text{Ag}_3\text{PO}_4/\text{SnO}_2$, indicating that SnO_2 greatly enhanced the stability of Ag_3PO_4 photocatalyst. Furthermore, the photocatalytic stability of $\text{Ag}_3\text{PO}_4/\text{SnO}_2$ was investigated by recycling in the repeated MO degradation experiments. As shown in Fig. 5b, the MO dye is quickly bleached after every MO decomposition experiment, and $\text{Ag}_3\text{PO}_4/\text{SnO}_2$ photocatalysts are stable enough during the repeated experiments without exhibiting any significant loss of photocatalytic activity. Therefore, the as-prepared $\text{Ag}_3\text{PO}_4/\text{SnO}_2$ composites can work as effective photocatalysts for organic compounds degradation with good stability in the absence of electron acceptors.

Several reasons may account for the enhanced photocatalytic activity and stability of the $\text{Ag}_3\text{PO}_4/\text{SnO}_2$ photocatalysts. Firstly, the insoluble SnO_2 layer on the surface of Ag_3PO_4 can effectively

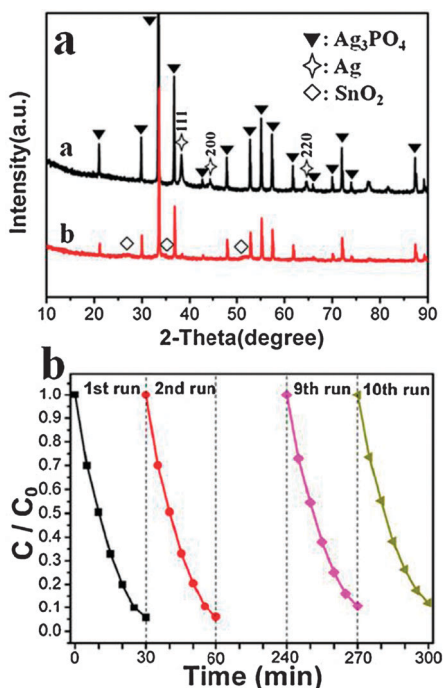


Fig. 5 (a) XRD patterns of Ag_3PO_4 and $\text{Ag}_3\text{PO}_4/\text{SnO}_2$ photocatalysts after 10 MO decomposition experiments. (b) The repeated bleaching of MO over recycled $\text{Ag}_3\text{PO}_4/\text{SnO}_2$ photocatalysts under visible light ($\lambda \geq 420$ nm).

protect the Ag_3PO_4 from dissolution in aqueous solution, thus the structural stability of $\text{Ag}_3\text{PO}_4/\text{SnO}_2$ can be greatly enhanced during the photocatalytic process.⁹ Secondly, as we know, SnO_2 has no absorption response to the visible light due to its wide band gap, therefore, the light absorption of $\text{Ag}_3\text{PO}_4/\text{SnO}_2$ composites was solely contributed by the Ag_3PO_4 component in the visible light photocatalysis experiments. However, the Ag_3PO_4 composites exhibited a more enhanced visible light photocatalytic efficiency than pure Ag_3PO_4 , which must be correlated to the complex band configuration of the $\text{Ag}_3\text{PO}_4/\text{SnO}_2$ photocatalysts. For $\text{Ag}_3\text{PO}_4/\text{SnO}_2$ photocatalysts, the conduction band and valence band potentials of SnO_2 are more positive than that of Ag_3PO_4 .^{7,22} Therefore, the photo-generated electrons in the Ag_3PO_4 can be easily transferred to the surface of the SnO_2 , and the photoinduced holes remain on the surface of Ag_3PO_4 , which promotes the effective separation of photoexcited electron-hole pairs and decreases the probability

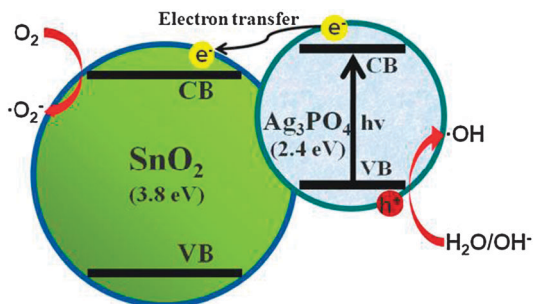


Fig. 6 Schematic model for the important roles of SnO_2 for the high photocatalytic activity and good stability in $\text{Ag}_3\text{PO}_4/\text{SnO}_2$.

of electron-hole recombination, as displayed in Fig. 6. Furthermore, the electronic acceptors like adsorbed O_2 can easily trap the electrons (transferred to the surface of SnO_2) to produce a superoxide anion radical $\cdot\text{O}_2^-$, which effectively protects Ag_3PO_4 semiconductors to avoid their photoreduction ($\text{Ag}^+ + e^- \rightarrow \text{Ag}$). Then the formed $\cdot\text{O}_2^-$ may either attack organic molecules or provide hydroxyl radical species ($\cdot\text{OH}$) by reacting with hydron and photogenerated electrons.²³ On the other hand, some of the photoinduced holes on the surface of Ag_3PO_4 can be trapped (the quantity of the SnO_2 in the composites is small and the SnO_2 layer on the surface of Ag_3PO_4 is not a compact layer) by OH^- to further produce $\cdot\text{OH}$ species, which is an extremely strong oxidant for the partial or complete mineralization of organic chemicals.²⁴ Based on the above aspects, it can be concluded that the proposed fabrication of $\text{Ag}_3\text{PO}_4/\text{SnO}_2$ is a successful and general strategy to develop highly active and stable photocatalysts under visible light irradiation.

In conclusion, we have developed a facile approach for the synthesis of $\text{Ag}_3\text{PO}_4/\text{SnO}_2$ composite photocatalysts. Significantly, compared with pure Ag_3PO_4 particles, the $\text{Ag}_3\text{PO}_4/\text{SnO}_2$ composite photocatalysts display enhanced photocatalytic activity and good structural stability for MO degradation under the irradiation of visible light. The insolubility of SnO_2 can effectively protect Ag_3PO_4 from dissolution. The $\text{Ag}_3\text{PO}_4/\text{SnO}_2$ composites improve the separation of photo-generated electron-hole pairs, thus enhancing the photocatalytic activity and avoid the photoreduction of Ag_3PO_4 . It can be expected that this kind of $\text{Ag}_3\text{PO}_4/\text{SnO}_2$ composite may provide a new approach for high performance novel catalyst design and fabrication towards new energy sources, green chemistry, and environmental issues.

Acknowledgements

This work is supported by the National Basic Research Program of China (973 Program) (No. 2012CB825800, 2010CB934500), National Natural Science Foundation of China (NSFC) (No. 51132006, 21073127, 21071104), A Foundation for the Author of National Excellent Doctoral Dissertation of P R China (FANEDD) (No. 200929), A Project Funded by the Priority Academic Program Development of Jiangsu Higher Education Institutions (PAPD) and a Project supported by the Natural Science Foundation of the Jiangsu Higher Education Institutions of China (Grant No. 11KJB150015).

Notes and references

- 1 A. Fujishima and K. Honda, *Nature*, 1972, **37**, 238.
- 2 H. Zhang, G. Chen and D. W. Bahnemann, *J. Mater. Chem.*, 2009, **19**, 5089.
- 3 Z. Kang, C. H. A. Tsang, N.-B. Wong, Z. Zhang and S.-T. Lee, *J. Am. Chem. Soc.*, 2007, **129**, 12090.
- 4 H. T. Li, X. D. He, Z. H. Kang, H. Huang, Y. Liu, J. L. Liu, S. Y. Lian, C. H. A. Tsang, X. B. Yang and S. T. Lee, *Angew. Chem., Int. Ed.*, 2010, **49**, 4430.
- 5 S. Linic, P. Christopher and D. B. Ingram, *Nat. Mater.*, 2011, **10**, 911.
- 6 Y. Liu, H. Ming, Z. Ma, H. Huang, S. Y. Lian, H. T. Li, X. D. He, H. Yu, K. M. Pan and Z. H. Kang, *Chem. Commun.*, 2011, **47**, 8025.

- 7 Z. G. Yi, J. H. Ye, N. Kikugawa, T. Kako, S. X. Ouyang, H. Stuart-Williams, H. Yang, J. Y. Cao, W. J. Luo, Z. S. Li, Y. Liu and R. L. Withers, *Nat. Mater.*, 2010, **9**, 559.
- 8 Y. Bi, S. Ouyang, N. Umezawa, J. Cao and J. Ye, *J. Am. Chem. Soc.*, 2011, **133**, 6490.
- 9 Y. P. Bi, S. X. Ouyang, J. Y. Cao and J. H. Ye, *Phys. Chem. Chem. Phys.*, 2011, **13**, 10071.
- 10 C. Chen, W. Ma and J. Zhao, *Chem. Soc. Rev.*, 2010, **39**, 4206.
- 11 H. Zhang, H. Ming, S. Lian, H. Huang, H. Li, L. Zhang, Y. Liu, Z. Kang and S.-T. Lee, *Dalton Trans.*, 2011, **40**, 10822.
- 12 S. Liu, J. M. Li, Q. Shen, Y. Cao, X. F. Guo, G. M. Zhang, C. Q. Teng, J. Zhang, Z. F. Liu, M. L. Steigerwald, D. S. Xu and C. Nuckolls, *Angew. Chem., Int. Ed.*, 2009, **48**, 4759.
- 13 Q. Wan and T. H. Wang, *Chem. Commun.*, 2005, 3841.
- 14 S. Ito, Y. Makari, T. Kitamura, Y. Wada and S. Yanagida, *J. Mater. Chem.*, 2005, **15**, 1106.
- 15 Z. Liu, D. D. Sun, P. Guo and J. O. Leckie, *Nano Lett.*, 2007, **7**, 1081.
- 16 C. Wang, Y. Zhou, M. Ge, X. Xu, Z. Zhang and J. Z. Jiang, *J. Am. Chem. Soc.*, 2010, **132**, 46.
- 17 R. Zhang, H. Wu, D. Lin and W. Pan, *J. Am. Chem. Soc.*, 2009, **92**, 2463.
- 18 M. L. Zhang, T. C. An, X. H. Hu, C. Wang, G. Y. Sheng and J. M. Fu, *Appl. Catal., A*, 2004, **260**, 215.
- 19 J. King, Q. Kuang, Z.-X. Xie and L.-S. Zheng, *J. Phys. Chem. C*, 2011, **115**, 7874.
- 20 W.-W. Wang, Y.-J. Zhu and L.-X. Yang, *Adv. Funct. Mater.*, 2007, **17**, 59–64.
- 21 L. Zheng, Y. Zheng, C. Chen, Y. Zhan, X. Lin, Q. Zheng, K. Wei and J. Zhu, *Inorg. Chem.*, 2009, **48**, 1819–1825.
- 22 T. Niu, F. Huang, L. F. Cui, P. Huang, Y. L. Yu and Y. S. Wang, *ACS Nano*, 2010, **4**, 681.
- 23 A. F. Marye and T. D. Maria, *Chem. Rev.*, 1993, **93**, 341.
- 24 Y. Zheng, L. Zheng, Y. Zhan, X. Lin, Q. Zheng and K. Wei, *Inorg. Chem.*, 2007, **46**, 6980.